



Distribution and mRNA Expression of nAChRs in the Rat S1 and M1 Cortices After Electrical Stimulation of the Basal Forebrain

Necla BIRGUL IYISON¹, Begum DEVLET KILICKAP², Burcin DUAN SAHBAZ¹, Bige VARDAR², Burak GUCLU²

¹Bogazici University, Department of Molecular Biology and Genetics, Istanbul, Turkey

²Bogazici University, Institute of Biomedical Engineering, Istanbul, Turkey

This study has been presented as an oral presentation at the 17th Turkish Neuroscience Congress between 4 and 7 April 2019 at Trabzon, Turkey

Corresponding author: Necla BIRGUL IYISON ✉ birgul@boun.edu.tr

ABSTRACT

AIM: To study the changes in the distribution of and the transcriptional levels associated with $\alpha 4$ - and $\alpha 7$ -subtype nicotinic acetylcholine receptors (nAChRs) in the primary somatosensory (S1) and motor (M1) cortices of rats after electrical stimulation of the basal forebrain (BF).

MATERIAL and METHODS: Immunofluorescence (IF) analyses were performed on brain sections from 20 rats (experimental groups: controls, contralateral, and ipsilateral to BF stimulation). The nAChR receptor complexes were labeled with antibodies and counted (N) in the cortical layers of the hindlimb representation (S1HL), barrel field (S1BF), and M1. To determine the relative transcriptional mRNA levels, qRT-PCR was performed with tissue from the associated brain regions of 14 different animals in two groups, controls and BF stimulation.

RESULTS: For all three tested brain regions, N and D (density) of the $\alpha 7$ -subtype nAChR increased in both ipsilateral and contralateral hemispheres after BF stimulation. There was no change in N and D of the $\alpha 4$ subtype. Regardless of BF stimulation, N of both subtypes was lower in M1 compared to S1HL and S1BF, and D was highest in layers II-IV. BF stimulation had no significant effect on the relative mRNA levels of both receptor subtypes.

CONCLUSION: The results show an upregulation of the $\alpha 7$ -subtype nAChR as a result of BF stimulation, based on receptor-complex counts on IF images. However, this change was not reflected in mRNA levels, which suggest post-translational modifications. Overall, this study suggests structural changes from the effects of cholinergic projections to the somatosensory and motor cortices.

KEYWORDS: Somatosensory cortex, Nicotinic receptor, Cholinergic system, Basal forebrain, Motor cortex

ABBREVIATIONS: **ACh:** Acetylcholine, **AP:** Anterior-posterior, **BF:** Basal forebrain, **D:** Density, **DAPI:** 4'-6-diamidino-2-phenylindole dihydrochloride, **DV:** Dorsal-ventral, **EtOH:** Ethanol, **GAPDH:** Glyceraldehyde-3-phosphate dehydrogenase, **IF:** Immunofluorescence, **IgG:** Immunoglobulin G, **IP:** Intraperitoneal, **M1:** Primary motor cortex, **nAChR:** Muscarinic acetylcholine receptor, **ML:** Medial-lateral, **mPFC:** Medial prefrontal cortex, **N:** Number of receptor complexes, **nAChR:** Nicotinic acetylcholine receptor, **NaCl:** Sodium chloride, **NBM:** Nucleus basalis of Meynert, **PB:** Phosphate buffer, **PBTx:** Phosphate buffer with Triton X-100, **PBTxg:** Phosphate buffer with Triton X-100 and goat serum, **PC:** Pacinian corpuscles, **qRT-PCR:** Quantitative real-time polymerase chain reaction, **RA:** Rapidly adapting fibers, **ROI:** Region-of-interest, **RT:** Room temperature, **S1:** Primary somatosensory cortex, **S1BF:** Primary somatosensory barrel field, **S1HL:** Primary somatosensory cortex of the hindlimb, **SA-1:** Slowly adapting type 1 fibers, **SA-2:** Slowly adapting type 2 fibers, **T:** thickness

■ INTRODUCTION

Acetylcholine (ACh) is a key neurotransmitter that regulates several higher cortical functions, including attention, plasticity, and memory, through muscarinic (mAChR) and nicotinic (nAChR) receptors (37,38,73,77). Most of the cortical ACh is released by the terminals of cholinergic neurons whose cell bodies are located in the basal forebrain (BF), specifically in the nucleus basalis of Meynert (NBM). NBM has diffuse projections in the cortex (7,30,66,74). As a result, ACh has a widely distributed effect in the brain (26,34). The extracellular concentration of cortical ACh can give information about the level of activity in the cholinergic neurons. As a neuromodulator, ACh can change neuronal excitability and synaptic dynamics while regulating sensory processing (13,46,50,85). Lesions of the BF in animals cause attention and memory deficits (9,60), while BF stimulation increases cortical firing rates (3,30,33,71). It has been shown that electrical stimulation of the BF can regulate thalamocortical transmission to the auditory cortex in anesthetized rats (59).

The hindpaw representation of the rat primary somatosensory cortex (S1) has been relatively less studied compared to the barrel cortex (27). However, this area also receives inputs related to the mechanoreceptive fibers in the glabrous skin, and these fibers are similar in all mammals (5,36,40,41,49,52). In brief, there are four types of A β mechanoreceptive fibers in the glabrous skin: Pacinian (PC), rapidly adapting (RA), slowly adapting type 1 (SA-1), and slowly adapting type 2 (SA-2). These fibers mediate the sense of discriminative touch and are associated respectively with Pacinian corpuscles (45,67), Meissner corpuscles (20,42,43), Merkel cell-neurite complexes (44,65), and Ruffini endings (25; see however Güçlü et al. [45] regarding glabrous skin). In the rat S1 cortex, there is submodality convergence regarding the skin afferents (15,51), which has also recently been reported in monkeys (69). Tactile neurons in the hindpaw representation of rat S1 cortex mostly respond at the onset of vibrotactile stimuli applied on glabrous skin, but they can be entrained at low frequencies (e.g., 5 Hz) as measured by the vector strength of spike phases (88). Recently, we found that BF stimulation changes the low-frequency synchronization of those neurons (87); spikes were more synchronized to 5 Hz tactile stimuli as a result of BF modulation. In that study, preliminary data further showed that ACh microinjection enhanced the modulatory effect of BF stimulation. However, tests with nAChR antagonists were not fully conclusive, which prompted us to undertake the current work regarding nAChRs.

nAChRs are pentameric structures which consist of a combination of subunits α 2- α 10 and β 2- β 4. In the mammalian cortex, two main subtypes are expressed: the low-affinity homomeric α 7-subtype located both pre- and postsynaptically and the high-affinity heteromeric α 4 β 2-subtype located on presynaptic sites (2,8,11,64,79), including thalamocortical fibers (55,76). Both are considered to be critical for learning, memory, and attention (53,54). nAChRs regulate synaptic transmission at both thalamocortical synapses and intracortical synapses (17,55,63,90). The diversity in their functional properties is probably a result of the subunit composition (1).

Tian et al. (82) studied the effects of cholinergic excitation in the mouse primary motor (M1) cortex, S1 cortex, and medial prefrontal cortex (mPFC), which is implicated in the top-down control of attention. In particular, layer VI was investigated as the main input for cholinergic innervation, and by using antagonists, the receptor contributions to the responses were varied in the different regions. In the S1 cortex, the contributions of nAChR-mediated and mAChR-mediated responses were 63% and 37%, respectively. On the other hand, the contribution of nAChRs in the M1 cortex and mPFC were 83% and 91%, respectively. Given these results within the tested regions, it may be conjectured that nAChRs are relatively more important in top-down modulation of attentional behavior, and mAChRs may have a greater role in the sensorimotor component of attention. On the contrary, the nAChR-mediated response is stronger in the S1 cortex. Although many studies are investigating the distribution of nAChR receptors in the brain (11,18,25,48,82,89), they do not provide detailed information regarding their specific locations within the S1 cortex as well as laminar distribution, which would be helpful data to correlate with neurophysiological experiments.

Since the contribution of nAChRs to somatosensory processing is not fully established, especially in the hindlimb area of rat S1 cortex (S1HL; slightly larger than the hindpaw representation; see Chapin and Lin [15]), we hypothesized that BF stimulation may induce molecular and anatomical changes in the related area. Laminar distribution of receptor complexes with α 4 and α 7 subunits was studied with immunofluorescence (IF) in rats after BF stimulation. Additionally, a real-time quantitative polymerase chain reaction (qRT-PCR) was performed to test whether changes in messenger RNA (mRNA) levels were associated with BF stimulation. The barrel cortex (S1BF) and M1 cortex were also studied for comparison. The current results show that BF stimulation increases the number of nAChR complexes, including the α 7 subunit, but not of those including the α 4 subunit in both hemispheres regardless of the area studied. However, mRNA expression levels were not influenced by BF stimulation for both receptor subtypes, which suggests that the changes were probably post-translational. The preliminary results of this study were presented as an abstract (21).

■ MATERIAL and METHODS

Animals and Surgery

Twenty adult Wistar albino rats (7 male and 13 female, weight range: 192 – 407 g) were used for IF investigations (7 controls, 6 for contralateral to BF stimulation, 6 for ipsilateral to BF stimulation, 1 for both contralateral and ipsilateral to BF stimulation). 14 adult Wistar albino rats (3 male and 11 female, weight range: 215 – 456 g) were used for qRT-PCR investigations (7 controls, 7 for both contralateral and ipsilateral to BF stimulation). Except for the 7 controls in the qRT-PCR procedure, the other 27 rats mentioned above were included in the current study after neurophysiological data collection under anesthesia in other studies (39,87) to minimize animal use. All experiments were approved by the Bogazici

University Institutional Ethics Committee for the Local Use of Animals in Experiments (Date: 16.03.2017, No: 2017/1). Before transcatheter perfusion, all animals were under surgical anesthesia (65-100 mg/kg ketamine and 10 mg/kg xylazine IP) as confirmed by palpebral and pedal reflexes. Perfusion was performed with 0.9% NaCl followed by 4% paraformaldehyde (1.04005.100; Merck, NJ, USA) at pH 7.4. The brains were quickly removed and post-fixed for 24 h in neutral buffered paraformaldehyde/sucrose solution (4%/20%) at 4°C.

BF Stimulation

The details of craniotomy for BF stimulation are given in Vardar and Guclu (87). Custom-made bipolar tungsten (World Precision Instruments, Sarasota, FL, USA) electrodes were placed at NBM (ML +2.4 mm, AP -1.3 mm, DV +6.8 mm) based on the stereotaxic atlas (68), and previous studies (32). Biphasic charge-balanced electrical current pulses (pulse duration: 0.5 ms, amplitude: 50 μ A) were applied by using an isolated current source (model 2300; A-M Systems, Sequim, WA, USA) controlled by the digital outputs of a multi-purpose data acquisition card (USB-6251; National Instruments, Austin, TX, USA). The timing of the stimulation protocol was programmed in MATLAB (Version R2008a; The MathWorks, Natick, MA, USA). A total of 3000 pulses were applied for each animal subject to BF stimulation (87).

Immunofluorescence (IF) Protocol for nAChRs

Post-fixed brains were washed with phosphate buffer (PB) that contains Triton X-100 (PBTx) (Sigma-Aldrich, St. Louis, MO, USA) 6 times each for 30 min. The brains were sectioned coronally at 50 μ m thickness by using a vibratome (VT1000S; Leica Biosystems, Wetzlar, Germany). Sections were rinsed with PBTx in a multi-well plate for further processing. For blocking, sections were kept in PBTx with 10% normal goat serum (PBTxg) for 1 h at room temperature (RT). Then, the sections were incubated in 150 μ L primary antibody solution (diluted 1:50 in PBTx) for 24 h at 4°C. Rabbit polyclonal antibodies were used for the α 4 nAChR subtype (sc-5591; Santa Cruz Biotechnology, Dallas, TX, USA) and the α 7 nAChR subtype (sc-5544; Santa Cruz Biotechnology). Afterward, the sections were rinsed 3 times with PBTx (each 30 min). 150 μ L of the secondary antibody solution (diluted 1:50 in PBTxg) was added and the sections were incubated at 4°C in darkness for 12 h. The secondary antibody was a goat anti-rabbit IgG (H+L) with Alexa Fluor 594 (A-11012; Thermo Fisher Scientific, Waltham, MA, USA). Finally, incubated sections were rinsed 3 times with fresh PB each for 30 min, and then in 4 mM sodium carbonate solution (2 times, each 15 min) to lower background fluorescence. Sections were mounted with Fluoroshield (F6182; Sigma-Aldrich, St. Louis, MO, USA) on gelatin-coated slides. Some of the serial sections were counterstained with DAPI (D9542; Sigma-Aldrich, St. Louis, MO, USA) before mounting for the analysis of cortical layer thicknesses. Each multi-well plate also contained control samples (no-primary, no-secondary). Additionally, we looked at positive/negative tissue controls from the cerebellum to verify the antibodies (22,61).

qRT-PCR Analysis

RNA samples were isolated from the entire S1HL, S1BF, and M1 regions separately (as determined in the anteroposterior axis) and from both hemispheres combined to increase the tissue sample. The tissues were kept in TRI Reagent[®] (Zymo Research, Irvine, CA, USA) and frozen at -80°C. Homogenization was performed in MagNa lyser (Roche Diagnostics, Rotkreuz, Switzerland). The homogenate was incubated at RT for 5 min for lysis. The lysate was centrifuged at 4 °C for 10 min at maximum speed (16,000 g). The supernatant was taken into a clean tube, 1:5 volume chloroform was added and mixed via vortex shaker for 20 s. The tube was incubated at RT for 2-3 min and centrifuged at 10,000 g for 18 min. The aqueous part was taken into a clean tube, 1:1 volume of 100% EtOH was added and mixed via inverting the tube. The mixture was centrifuged in Zymo-Spin[™] IIICG columns (Zymo Research, Irvine, CA, USA) for 1 min. The remaining protocol of Direct-zol[™] RNA Miniprep Plus (Zymo Research, Irvine, CA, USA) was applied according to the recommendations of the manufacturer.

The RNA samples were reverse transcribed into cDNA by using SensiFAST cDNA Synthesis Kit (BIO-65054; Boline – Meridian Life Science, Memphis, TN, USA) according to the recommended protocol of the manufacturer. cDNA was diluted 1:2 and 1 μ L of this was used for each qRT-PCR reaction.

LightCycler[®] 480 SYBR Green I Master (Roche Diagnostics, Rotkreuz, Switzerland) was used according to the protocol of the manufacturer. The reaction was adjusted to 35 cycles. Rat primers for nAChR α 4 (Forward TGACGTGGAC-GAGAAGAACC, Reverse AGTTGGTCCACACGGCTATG) and nAChR α 7 (Forward CAAGGCGAGTTCCAGAGGAG, Reverse CGCTCATCAGCACTGTTATAGA) were utilized together with beta-actin (Forward AGATCAAGATCATTGCTCCTCT, Reverse ACGCAGCTCAGTAACAGTCC) and GAPDH (Forward AGTGCCAGCCTCGTCTCATA, Reverse GATGGTGATGG-TTTCCCGT) as the reference genes. Amplification factors of each primer couples were calculated, and relative gene expression was analyzed with regard to the two reference genes.

Imaging and Statistical Analyses

The serial coronal sections were obtained from the brain regions S1HL, S1BF, and M1 based on the boundaries in the anteroposterior axis as indicated in the atlas (68). All length measurements (including the region boundaries) were normalized according to the bregma-lambda distance of each rat and the atlas rat. For the histological analyses and counting of labeled nicotinic receptor complexes, three sections from the middle of the serial-section set were used in each brain region. The averages of these three counts were used for statistical analyses. The measurement sections were not adjacent because of controls, different antibody staining, and DAPI staining; they were interleaved between the treatments. However, cortical layer thicknesses (T) were determined in the DAPI-stained section adjacent to each measurement section. The sections were imaged under a fluorescence microscope (DM2500; Leica Microsystems, Wetzlar, Germany) with a camera (DFC310FX; Leica), and initially studied in LAS (Leica Ap-

plication Software). A region-of-interest (ROI) with a width of 600 µm and approximately parallel to the cortical surface was determined for each coronal measurement section. The images were saved at ×200 magnification with two excitation lights (filter cubes: N2.1 and I3), and the antibody-labeled receptor complexes in the ROI were counted for each cortical layer in a semi-automatic manner by using Fiji (Ver. 2.0.0; <http://fiji.sc/>) image processing software. Only structures with emission under N2.1 filter and which had higher brightness than twice the background brightness were counted. We did not look for a one-to-one correspondence between labeled structures and labeled cells. That is to say, there could be more than one labeled receptor complex in a labeled cell, and a labeled structure could be part of more than one cell.

The numbers of counted α4- and α7-subtype nAChR complexes (N) were analyzed as dependent variables in repeated-measures ANOVA by using SPSS Ver. 22 (IBM, Armonk, NY, USA). The brain region (S1HL, S1BF, and M1) was a within-subject factor, and the experimental condition (control, contralateral to BF stimulation, ipsilateral to BF stimulation) was a between-subject factor. Similar analyses were performed for the densities of α4- and α7-subtype nAChR complexes (i.e. D = N/T) as dependent variables. For the comparison of mRNA levels, both hemispheres were represented in the data to maximize the amount of tissue sample in qRT-PCR; therefore, a repeated measures ANOVA was performed with the brain region as the within-subject factor and the experimental condition (control vs. BF stimulation) as the between-subject factor. Post-hoc tests were done in SPSS with Bonferroni correction for multiple comparisons if a factor was found to be significant (p<0.05). The cortical layer thickness was analyzed by repeated-measures ANOVA as a dependent variable, and it was also included as a factor in the final step of IF analyses.

RESULTS

General Histological Observations

The cortical layer thicknesses obtained from the three tested rat brain regions are shown in Table I as means across subjects (all included in the IF analyses) and standard errors. These values are from DAPI-stained sections, but they are consistent with our previous work (91), and other studies reported in the literature (14,23). The total cortical thickness was found to be highest in S1BF (1623 µm) and lowest in S1HL (1567 µm); M1 cortex had an intermediate value (1594 µm). Indeed, the brain region had a significant main effect in repeated-measures ANOVA (p=0.002). Post-hoc tests showed that only the difference between S1BF and S1HL thicknesses was significant. Additionally, the thickness changed significantly depending on the layer as expected (p<0.001). However, there was also a significant interaction between the region and the layer (p<0.001). The thicknesses increased monotonically toward the deeper layers in both S1HL and S1BF, except in M1. As expected from standard neuroanatomy, layer IV is the main input layer in sensory cortices, but it is much thinner in M1. Similarly, layers II-III are the main processing layers; they are particularly prominent in S1BF, which has a major afferent input related to the whiskers. On the other hand, M1 as the

motor output layer has the most distinctive layer V compared to other tested regions.

Samples of IF images are shown for the α4-subtype (Figure 1A) and the α7-subtype (Figure 1B) of nAChRs after ipsilateral BF stimulation. The upper panels are the images with the correct filter setting (N2.1) and show the supragranular layers of S1HL. The immunoreactivity was robust for both tested antibodies, and staining could be observed at the cell perikarya and dendritic processes. The middle panels were obtained with a different filter setting (I3) to test for autofluorescence. On the overlaid images (e.g., bottom panels), only structures with a single-color emission (red, but not yellow) were counted (see Material and Methods). The bottom panels are from layer V and show the staining of large and distinct pyramidal neurons. The box indicates the ROI used for counting. The mediolateral width of the box is fixed at 600 µm as mentioned above. The vertical height represents the thickness of layer V (as verified in adjacent DAPI-stained sections) in these examples.

Effects of BF Stimulation on the Distribution of nAChR Complexes

Figure 2A, B shows the number of receptor complexes (N) and their densities based on layer thicknesses (D) for data pooled across brain regions and cortical layers. In repeated measures ANOVA, a main effect for the experimental condition was found only for the α7-subtype nAChR (N: p=0.001, D: p<0.001). Post-hoc tests showed that both the contralateral and ipsilateral hemispheres with BF stimulation had increased N and D as compared to the controls. There was no significant effect of BF stimulation on the N and D of the α4-subtype nAChRs, although a slightly increasing trend was also observed.

There was a significant main effect of brain region on N for both subtypes (α4: p=0.003, α7: p<0.001). Specifically, N was lower in M1 compared to S1HL and S1BF (Figure 3A, C). However, a significant difference could not be found between the N values from S1HL and S1BF. On the other hand, there was no main effect of brain region on D for the α7 subtype (Figure 3D). This factor was significant for D from the α4 subtype (p=0.040). Post-hoc tests showed that S1HL had higher D compared to both S1BF and M1 (Figure 3B). No interaction

Table I: Cortical Layer Thicknesses in S1HL, S1BF, and M1 of rat cortex. All Subjects from the IF Study are Included. Mean ± Standard Error

Cortical layer	S1HL (µm)	S1BF (µm)	M1 (µm)
I	102.0 ± 8.1	83.2 ± 6.2	94.0 ± 6.5
II	122.9 ± 6.3	153.8 ± 14.3	109.8 ± 6.1
III	146.9 ± 7.3	186.6 ± 18.2	128.3 ± 5.1
IV	168.9 ± 7.4	201.8 ± 11.9	108.0 ± 6.9
V	402.8 ± 21.8	372.5 ± 21.4	493.4 ± 39.6
VI	623.2 ± 69.4	625.1 ± 67.0	660.3 ± 60.3
Total	1566.7 ± 88.7	1623.0 ± 97.8	1593.8 ± 89.0

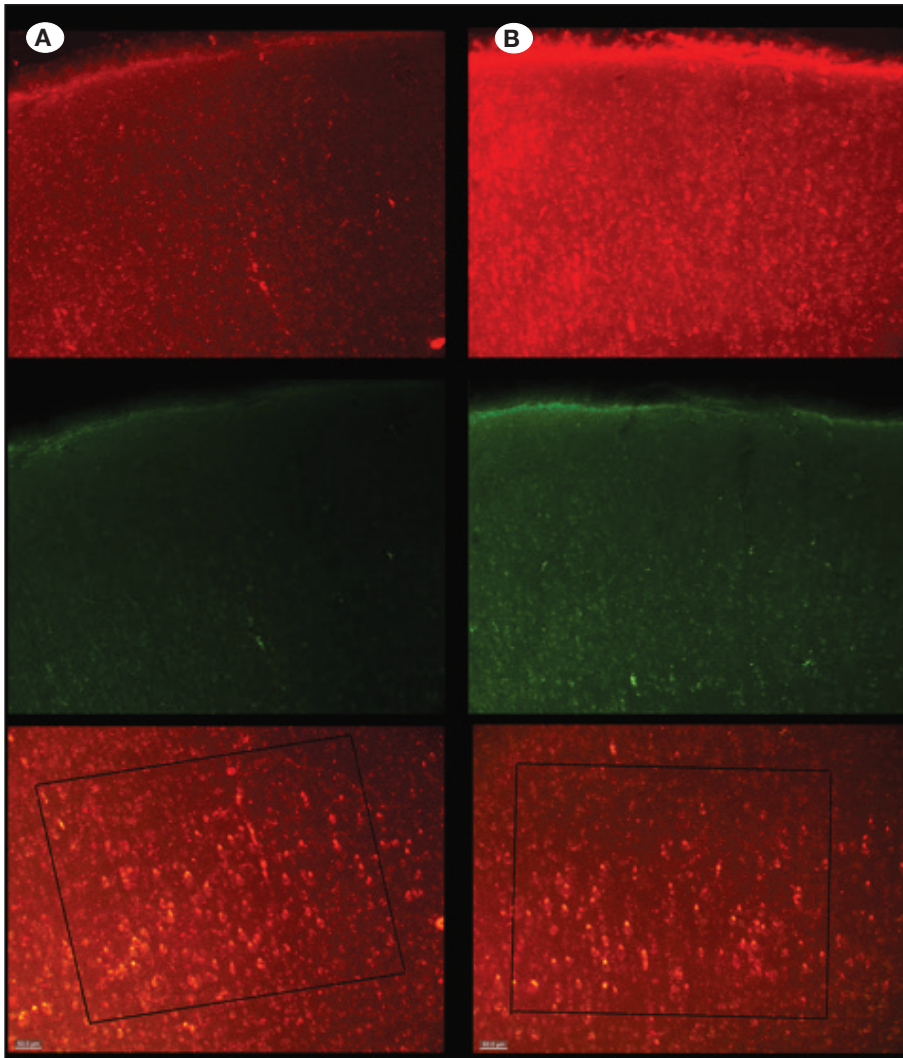


Figure 1: Immunofluorescence images of (A) $\alpha 4$ -subtype and (B) $\alpha 7$ -subtype nAChRs in the rat S1HL cortex after ipsilateral BF stimulation. Upper panels show results using the correct excitation/emission filter (N2.1) and show immunoreactivity related to the labeled receptor complexes. Middle panels show results with filter I3 used for testing autofluorescence. Bottom panels are overlaid images with ROI marked with a rectangle (layer V for these images) for counting receptor complexes. Only structures with a single-color emission (red, but not yellow) were counted. Magnification: $\times 200$. Scale bars: $50 \mu\text{m}$.

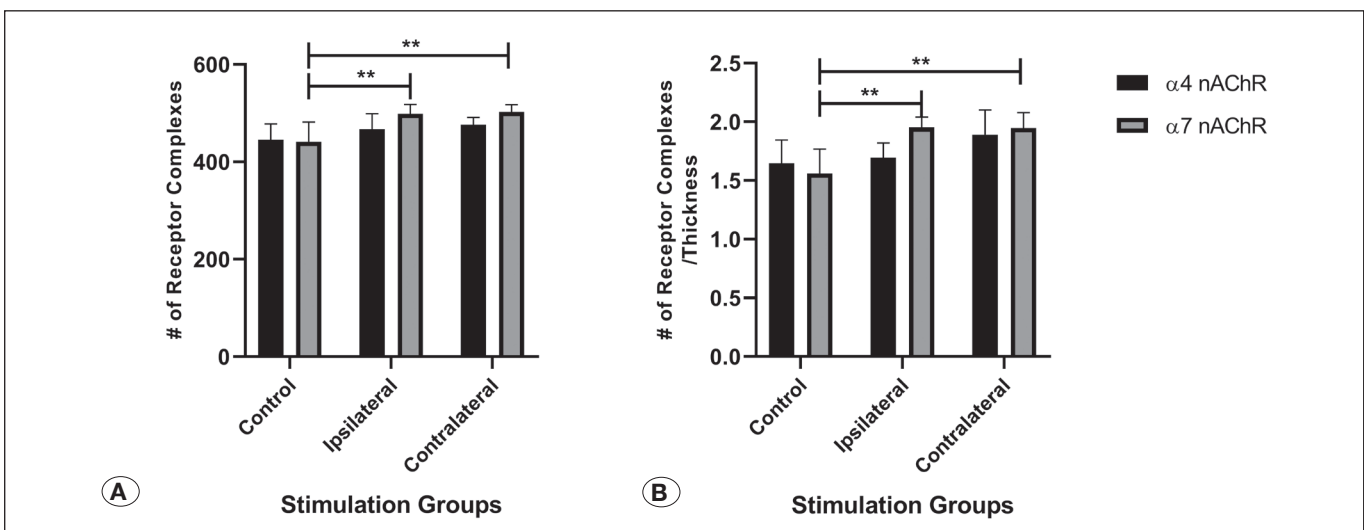


Figure 2: Total number (A) and the density (B) of $\alpha 4$ -subtype and $\alpha 7$ -subtype nAChR complexes with data pooled from S1HL, S1BF, and M1. Density values were found by dividing each count obtained in a cortical layer by the layer thickness. Control: no BF stimulation, ipsilateral: data from the same hemisphere of the BF stimulation, contralateral: data from the opposite hemisphere of BF stimulation. Error bars are standard deviations. *: $p < 0.05$, **: $p < 0.01$.

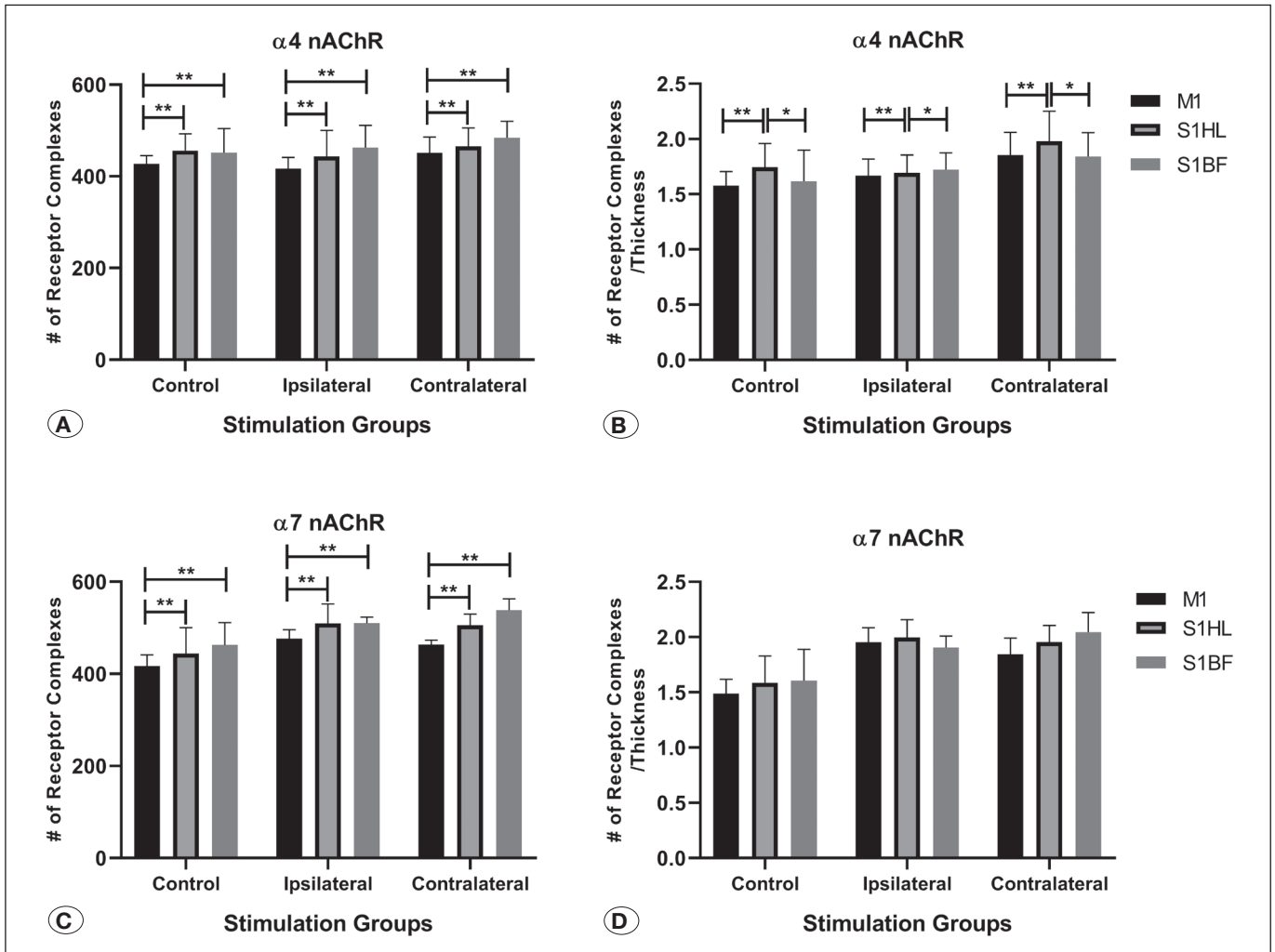


Figure 3: The number (A, C) and the density (B, D) of $\alpha 4$ -subtype and $\alpha 7$ -subtype nAChR complexes in S1HL, S1BF, and M1. Density values were found by dividing each count obtained in a cortical layer by the layer thickness. Layer data were pooled for brevity. Control: no BF stimulation, ipsilateral: data from the same hemisphere of the BF stimulation, contralateral: data from the opposite hemisphere of BF stimulation. Error bars are standard deviations. *: $p < 0.05$, **: $p < 0.01$.

effects could be found between the experimental condition and the brain region on either N or D for both subtypes.

When the cortical layer was introduced as a factor to repeated measures ANOVA, the conclusions regarding BF stimulation and brain region were similar to those presented above. Additionally, there were significant main effects of cortical layer on both N and D and for both subtypes (all $p < 0.001$). In fact, there was a significant interaction between cortical layer and brain region on N ($p = 0.001$ for both subtypes). For S1HL and S1BF, there was a consistent and a statistically significant increase in the number of receptor complexes (both subtypes) from approximately 100 to 1000 with differing depths, i.e., from layer I to layer VI. However, in M1, Ns of both subtypes stayed in the range of 200-300 for the layers II-IV. The layer \times region interaction on D was significant for the $\alpha 4$ subtype ($p = 0.022$) but not for the $\alpha 7$ subtype. The D of the $\alpha 4$ subtype was high (~2 per μm thickness of ROI) for the layers II-IV in S1HL and M1 but significantly lower in S1BF. D varied 1.2-1.9 in S1BF

but was 1.1-2.2 in S1HL and M1 across all layers. In all tested regions, D was the highest in cortical processing and input layers (II-IV). The main effect of the cortical layer on D for the $\alpha 7$ subtype followed a similar trend: D was the lowest in layer I and highest in layers II-IV. It is important to note, however, that the experimental condition, i.e., BF stimulation, did not interact with the layer factor for either N or D from both subtypes. In other words, the stimulation effect described above was independent of the brain region and cortical layer.

Effects of BF Stimulation on mRNA Levels

Since there was a significant difference in the number and density of $\alpha 7$ -subtype nAChR complexes after BF stimulation, we studied whether this may correspond to regulation at the level of mRNA expression. Repeated measures ANOVA performed on data from different rats showed that there is no significant effect of BF stimulation on the relative levels of mRNA related to both receptor subtypes (Figure 4B). We

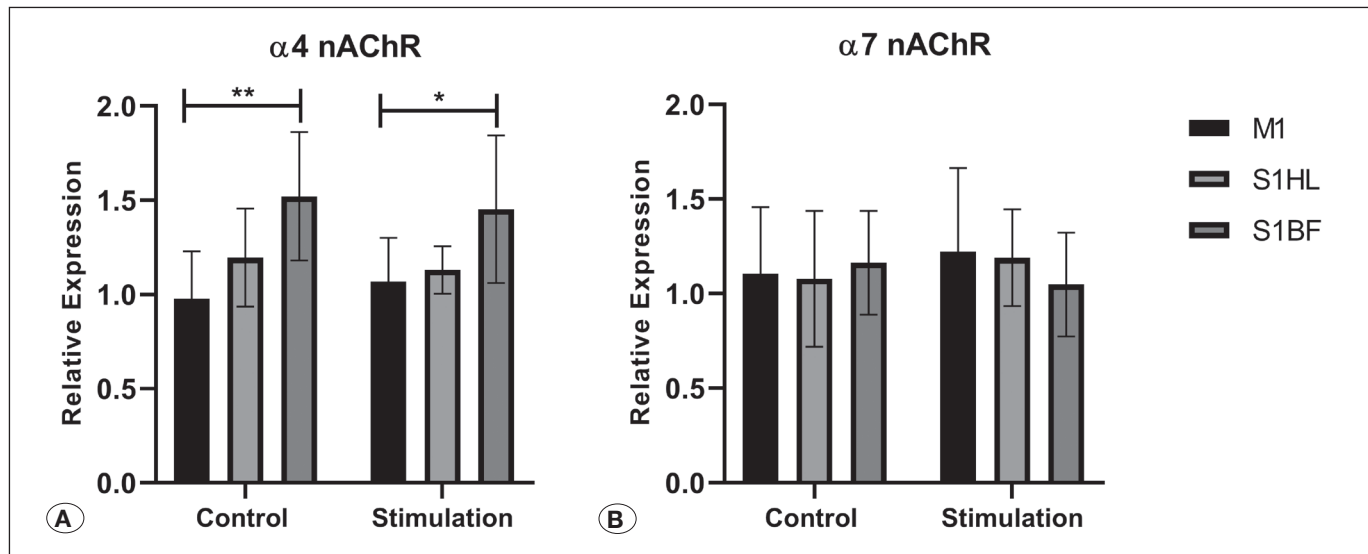


Figure 4: Relative mRNA expression levels of (A) α4-subtype and (B) α7-subtype nAChRs in S1HL, S1BF, and M1 without and after BF stimulation. Both hemispheres were included in tissue samples. The expression levels were obtained with regard to two reference genes and normalized to the control group results. Error bars are standard deviations. *: $p < 0.05$, **: $p < 0.01$.

found a significant effect of a brain region only for the α4 subtype ($p=0.016$). Specifically, post-hoc tests showed that M1 had lower levels than S1BF. S1HL had also marginally higher levels than M1 ($p=0.051$). There was no difference according to brain regions for the α7 subtype.

DISCUSSION

nAChRs are widely distributed in the mammalian brain and they have a role in both neuromodulation and neurotransmission (70). The mutations in genes that code for the α4 and β2 subunits of nAChRs can be responsible for some forms of autosomal frontal lobe epilepsy (16,19,81). Mutant receptors increase the sensitivity to ACh compared with normal receptors by enhancing neuronal excitability. Therefore, the excitation-inhibition balance is disturbed, which is the cause of epileptic seizures (72). In contrast, temporal lobe seizures originate from limbic structures and generally have self-limiting mechanisms. However, when their self-limiting mechanisms fail, seizures can last over 5 min or be repeated without recovery, which is defined as status epilepticus (SE) (84). SE can cause damage in limbic and subcortical structures, and significant cholinergic neuron loss in the BF is also characteristic in SE (6,31). BF is a part of the limbic system (31), and cholinergic modulation of the cerebral cortex is largely controlled by the BF (4,56,57). BF is important not only for epilepsy but also for dementia. Because there is no effective treatment for dementia, deep brain stimulation (DBS) could be an alternative treatment. Alzheimer’s disease (AD) and Parkinson’s disease dementia (PDD) are characterized by the loss of cholinergic neurons in the nucleus basalis of Meynert of the basal forebrain. Several post-mortem human studies show that cell loss is almost 96% for NBM neurons in both AD and PDD patients (12,24,29). However, targeting of the NBM for DBS has challenges from a surgical perspective because the NBM does not have

clear anatomic boundaries. In the first human study that targeted the NBM (86), the stimulation electrode was placed into the left NBM via the frontal approach for the patient with moderate AD. No difference in cognition was reported. However, cortical glucose metabolic activity was preserved in the ipsilateral temporal and parietal lobes compared to other cortical regions. Subsequently, the dorsolateral portion of NBM and sub-thalamic nucleus were stimulated bilaterally in a patient with slowly progressive PDD (28). The effects of BF stimulation were noticed in the first few weeks. Cognitive decline that was observed before the DBS did not continue following the NBM stimulation during the 13-week observation period. Instead, improvement in attention, concentration, and alertness was observed after the NBM stimulation. A recent study (35) targeted the intermediate part of the NBM in six patients with PDD. No improvements in cognitive abilities was observed. These variations in results of human DBS studies for dementia could be explained by the difference in DBS electrode placement.

We specifically targeted NBM, which is the source of ACh in the cerebral cortex, for electrical stimulation. Previous animal studies on the electrical stimulation of BF showed that sensory processing is affected mostly by cholinergic inputs as well as other receptor influences. We examined the possible effects of BF stimulation on the distribution of nAChRs. We have recently found that the synchronicity of tactile neurons in S1HL to low-frequency skin vibrations is improved after BF stimulation, and ACh microinjection in the same cortical area further enhanced this modulatory effect (87). nAChR-mediated responses are stronger in S1 cortex as compared to mAChR-mediated responses (82). In the current research, we studied the laminar distribution of α4- and α7-subtype nAChRs by IF after BF stimulation. The results show a robust increase in the number and density (i.e., count normalized by layer thickness in the ROI) of the α7 subtype

after BF stimulation. However, qRT-PCR performed on different animals with the same stimulation protocol suggests that this change is not at the level of mRNA expression. BF stimulation did not produce appreciable changes in relative expression levels. Nevertheless, the changes at the receptor level suggest structural effects of cholinergic projections to the somatosensory and motor cortices.

The cortical layer thickness measurements obtained with DAPI staining and our antibody-labeling of nAChRs are consistent with general neuroanatomical literature. It was reported that both $\alpha 4$ - and $\alpha 7$ - subtype nAChRs are mainly found in layer III and IV of S1 and layer III and V of M1, especially the $\alpha 4$ subtype (11,22,58,78). Moreover, it was recently reported that primary sensory areas including S1 in the human cortex have a very high density of the $\alpha 4$ subtype (92). Although the number of receptor complexes increased in deeper layers of our rat data, we found that layers II-IV had the highest densities, somewhat consistent with the above-cited studies. These layers are general processing (II-III) and input (IV) layers of the cortex. In the human study by Zilles and Palomero-Gallagher (92), the granular layer of S1, i.e., layer IV, had an exceptionally high density of the $\alpha 4$ subtype, highlighting the importance of cholinergic modulation at the sensory input stage.

Interestingly, the hindpaw representation of the rat S1 cortex also overlaps with the motor cortex (47,62). We found that S1HL had thicker layers I-IV than those in M1, but thinner layers V-VI than those in M1. Apparently, S1HL is intermediate between S1BF and M1 with respect to anatomical properties. When the data are pooled across the layers, the number of receptor complexes (both subtypes) was lower in M1 compared to S1HL and S1BF. On the other hand, S1HL had the highest density of the $\alpha 4$ subtype in general. All three tested regions had similar densities of the $\alpha 7$ subtype. More importantly, however, the relative distribution of receptors in terms of count or density did not change along with the layers or across the tested regions because of BF stimulation. The upregulation of the $\alpha 7$ subtype was consistent across these anatomical regions.

Local application of AChR agonist or ACh itself can affect the excitability of neurons and synaptic properties (10,75,79), but there are still many unknowns regarding the exact role of nAChRs. The effect of one-sided BF stimulation was similar for both hemispheres in our study. Therefore, we could include tissue from both hemispheres in the qRT-PCR analyses, and this also increased the reliability of the method. Since we could not obtain a significant difference in the mRNA transcriptional expression level afterward because of BF stimulation, the increase in the immunoreactivity with respect to the $\alpha 7$ receptor subtype might have occurred because of receptor trafficking such as internalization or desensitization or degradation processes, which need further investigation (80). Additionally, the differences between two receptor subtypes may indicate different cholinergic networks in the related areas of the cortex.

■ CONCLUSION

Previous studies regarding the distribution of nAChR in the brain do not provide detailed information for the specific areas and layers within the S1 cortex. The current study presents the number and density of nAChR complexes obtained by the standard IF technique and is useful for future correlation with neurophysiological data and computational models. Specifically, we hypothesized that BF stimulation may induce molecular and anatomical changes in the hindlimb area of the rat S1 cortex. BF stimulation increased the number and density of nAChR complexes, including the $\alpha 7$ subunit but not of those including the $\alpha 4$ subunit, in both hemispheres regardless of the areas (S1HL, S1BF, M1) studied. On the other hand, the relative mRNA levels of both receptor subtypes, measured by qPCR, were not affected. Therefore, the changes observed in IF are attributed to post-translational modifications.

■ ACKNOWLEDGMENTS

This work was supported by a Bogazici University Research Fund (BAP no. 17XP2) grant to Dr. Guclu.

We thank Batuhan Babür for help during the IF image analyses. We also appreciate the helpful comments by Assoc. Prof. Asli Kumbasar (Istanbul Technical University) and Assist. Prof. Daniela Schulz (Bogazici University) on the preliminary results of this study.

■ REFERENCES

1. Albuquerque EX, Pereira EFR, Alkondon M, Rogers SW: Mammalian nicotinic acetylcholine receptors: from structure to function. *Physiol Rev* 89:73-120, 2009
2. Arroyo S, Bennett C, Hestrin S: Nicotinic modulation of cortical circuits. *Front Neural Circuits* 8:1-6, 2014
3. Avery MC, Dutt N, Krichmar JL: Mechanisms underlying the basal forebrain enhancement of top-down and bottom-up attention. *Eur J Neurosci* 39:852-865, 2014
4. Ballinger EC, Ananth M, Talmage DA, Role LW: Basal forebrain cholinergic circuits and signaling in cognition and cognitive decline. *Neuron* 91:1199-1218, 2016
5. Bensmaia SJ, Leung YY, Hsiao SS, Johnson KO: Vibratory adaptation of cutaneous mechanoreceptive afferents. *J Neurophysiol* 94:3023-3036, 2005
6. Biagioni F, Gaglione A, Giorgi FS, Bucci D, Moyanova S, De Fusco A, Madonna M, Fornai F: Degeneration of cholinergic basal forebrain nuclei after focally evoked status epilepticus. *Neurobiol Dis* 121:76-94, 2019
7. Biesold D, Inanami O, Sato A, Sato Y: Stimulation of the nucleus basalis of Meynert increases cerebral cortical blood flow in rats. *Neurosci Lett* 98:39-44, 1989
8. Bloem B, Schoppink L, Rotaru DC, Faiz A, Hendriks P, Mansvelter HD, van de Berg WDJ, Wouterlood FG: Topographic mapping between basal forebrain cholinergic neurons and the medial prefrontal cortex in mice. *J Neurosci* 34:16234-16246, 2014
9. Botly LCP, De Rosa E: Impaired visual search in rats reveals cholinergic contributions to feature binding in visuospatial attention. *Cereb Cortex* 22:2441-2453, 2012

10. Broide RS, Robertson RT, Leslie FM: Regulation of alpha7 nicotinic acetylcholine receptors in the developing rat somatosensory cortex by thalamocortical afferents. *J Neurosci* 16:2956-2971, 1996
11. Broide RS, Winzer-Serhan UH, Chen Y, Leslie FM: Distribution of $\alpha 7$ nicotinic acetylcholine receptor subunit mRNA in the developing mouse. *Front Neuroanat* 13:76, 2019
12. Candy JM, Perry RH, Perry EK, Irving D, Blessed G, Fairbairn AF, Tomlinson BE: Pathological changes in the nucleus of meynert in alzheimer's and parkinson's diseases. *J Neurol Sci* 59:277-289, 1983
13. Castro-Alamancos MA: Absence of rapid sensory adaptation in neocortex during information processing states. *Neuron* 41:455-464, 2004
14. Chapin JK: Laminar differences in sizes, shapes, and response profiles of cutaneous receptive fields in the rat SI cortex. *Exp Brain Res* 62:549-559, 1986
15. Chapin JK, Lin CS: Mapping the body representation in the SI cortex of anesthetized and awake rats. *J Comp Neurol* 229:199-213, 1984
16. Chen Y, Wu L, Fang Y, He Z, Peng B, Shen Y, Xu Q: A novel mutation of the nicotinic acetylcholine receptor gene CHRNA4 in sporadic nocturnal frontal lobe epilepsy. *Epilepsy Res* 83:152-156, 2009
17. Christophe E, Roebuck A, Staiger JF, Lavery DJ, Charpak S, Audinat E: Two types of nicotinic receptors mediate an excitation of neocortical layer I interneurons. *J Neurophysiol* 88:1318-1327, 2002
18. Dani JA: Overview of nicotinic receptors and their roles in the central nervous system. *Biol Psychiatry* 49:166-174, 2001
19. De Fusco M, Becchetti A, Patrignani A, Annesi G, Gambardella A, Quattrone A, Ballabio A, Wanke E, Giorgio C: The nicotinic receptor $\beta 2$ subunit is mutant in nocturnal frontal lobe epilepsy. *Nat Genet* 26:275-276, 2000
20. Devecioglu I, Guclu B: Asymmetric response properties of rapidly adapting mechanoreceptive fibers in the rat glabrous skin. *Somatosens Mot Res* 30:16-29, 2013
21. Devlet B, Vardar B, Babur B, Guclu B: Effects of basal forebrain stimulation on the distribution of nicotinic acetylcholine receptors with $\alpha 4/\alpha 7$ subunits in the somatosensory and motor cortex of rat brain. *International Journal of Experimental and Clinical Anatomy* 13 Suppl 1:30-31, 2019
22. Dominguez del Toro E, Juiz JM, Peng X, Lindstrom J, Criado M: Immunocytochemical localization of the alpha 7 subunit of the nicotinic acetylcholine receptor in the rat central nervous system. *J Comp Neurol* 349:325-342, 1994
23. Dykes RW, Lamour Y: An electrophysiological study of single somatosensory neurons in rat granular cortex serving the limbs: A laminar analysis. *J Neurophysiol* 60:703-724, 1988
24. Etienne P, Robitaille Y, Wood P, Gauthier S, Nair NP, Quirion R: Nucleus basalis neuronal loss, neuritic plaques and choline acetyltransferase activity in advanced Alzheimer's disease. *Neuroscience* 19:1279-1291, 1986
25. Fabian-Fine R, Skehel P, Errington ML, Davies H a, Sher E, Stewart MG, Fine A: Ultrastructural distribution of the $\alpha 7$ nicotinic acetylcholine receptor subunit in rat hippocampus. *J Neurosci* 21:7993-8003, 2001
26. Fournier GN, Semba K, Rasmusson DD: Modality and region-specific acetylcholine release in the rat neocortex. *Neuroscience* 126:257-262, 2004
27. Fox K: *Barrel Cortex*. Leiden: Cambridge University Press, 2008
28. Freund HJ, Kuhn J, Lenartz D, Mai JK, Schnell T, Klosterkoetter J, Sturm V: Cognitive functions in a patient with parkinson-dementia syndrome undergoing deep brain stimulation. *Arch Neurol* 66:781-785, 2009
29. Gaspar P, Gray F: Dementia in idiopathic Parkinson's disease. A neuropathological study of 32 cases. *Acta Neuropathol* 64:43-52, 1984
30. Gielow MR, Zaborszky L: The input-output relationship of the cholinergic basal forebrain. *Cell Rep* 18:1817-1830, 2017
31. Giorgi FS, Galgani A, Gaglione A, Ferese R, Fornai F: Effects of prolonged seizures on basal forebrain cholinergic neurons: Evidence and potential clinical relevance. *Neurotox Res* 38:249-265, 2020
32. Goard M, Dan Y: Basal forebrain activation enhances cortical coding of natural scenes. *Nat Neurosci* 12:1444-1449, 2009
33. Golmayo L, Nuñez A, Zaborszky L: Electrophysiological evidence for the existence of a posterior cortical-prefrontal-basal forebrain circuitry in modulating sensory responses in visual and somatosensory rat cortical areas. *Neuroscience* 119:597-609, 2003
34. Gotti C, Clementi F: Neuronal nicotinic receptors: From structure to pathology. *Prog Neurobiol* 74:363-396, 2004
35. Gratwicke J, Zrinzo L, Kahan J, Peters A, Beigi M, Akram H, Hyam J, Oswal A, Day B, Mancini L, Thornton J, Yousry T, Limousin P, Hariz M, Jahanshahi M, Foltynie T: Bilateral deep brain stimulation of the nucleus basalis of meynert for parkinson disease dementia: A randomized clinical trial. *JAMA Neurol* 75:169-178, 2018
36. Greenspan JD, Bolanowski SJ: The psychophysics of tactile perception and its peripheral physiological basis. In: Kruger L, (ed). *Pain and Touch*. San Diego, Ca: Academic Press, 1996: 25-104
37. Groleau M, Chamoun M, Vaucher E: Stimulation of acetylcholine release and pharmacological potentiation of cholinergic transmission affect cholinergic receptor expression differently during visual conditioning. *Neuroscience* 386:79-90, 2018
38. Gu Q: Neuromodulatory transmitter systems in the cortex and their role in cortical plasticity. *Neuroscience* 111:815-835, 2002
39. Guclu B, Duvan T: Evoked local field potentials from the hindpaw representation of rat SI cortex due to vibrotactile stimulation of the glabrous skin. Program No. 221.15. 2019 Neuroscience Meeting Planner. In: *Soc Neurosci 2019 Online*. Chicago, IL
40. Guclu B, Bolanowski SJ: Distribution of the intensity-characteristic parameters of cat rapidly adapting mechanoreceptive fibers. *Somatosens Mot Res* 20:149-155, 2003
41. Guclu B, Bolanowski SJ: Frequency responses of cat rapidly adapting mechanoreceptive fibers. *Somatosens Mot Res* 20: 249-263, 2003

42. Guclu B, Bolanowski SJ: Tristate markov model for the firing statistics of rapidly-adapting mechanoreceptive fibers. *J Comput Neurosci* 17:107-126, 2004
43. Guclu B, Bolanowski SJ, Pawson L: End-to-end linkage (EEL) clustering algorithm: A study on the distribution of Meissner corpuscles in the skin. *J Comput Neurosci* 15:19-28, 2003
44. Guclu B, Mahoney GK, Pawson LJ, Pack AK, Smith RL, Bolanowski SJ: Localization of Merkel cells in the monkey skin: An anatomical model. *Somatosens Mot Res* 25:123-138, 2008
45. Guclu B, Schepis EA, Yelke S, Yucesoy CA, Bolanowski SJ: Ovoid geometry of the Pacinian corpuscle is not the determining factor for mechanical excitation. *Somatosens Mot Res* 23:119-126, 2006
46. Himmelheber AM, Sarter M, Bruno JP: Increases in cortical acetylcholine release during sustained attention performance in rats. *Brain Res Cogn Brain Res* 9:313-325, 2000
47. Hummelsheim H, Wiesendanger M: Neuronal responses of medullary relay cells to controlled stretches of forearm muscles in the monkey. *Neuroscience* 16:989-996, 1985
48. Hurst R, Rollema H, Bertrand D: Nicotinic acetylcholine receptors: From basic science to therapeutics. *Pharmacol Ther* 137:22-54, 2013
49. Johansson RS, Vallbo AB: Tactile sensibility in the human hand: Relative and absolute densities of four types of mechanoreceptive units in glabrous skin. *J Physiol* 286:283-300, 1979
50. Kruglikov I, Rudy B: Perisomatic GABA release and thalamocortical integration onto neocortical excitatory cells are regulated by neuromodulators. *Neuron* 58:911-924, 2008
51. Lamour Y, Jobert A: Laminar distribution and convergence of deep and superficial peripheral inputs in the forelimb representation of rat SI somatosensory cortex. *J Physiol (Paris)* 78:158-162, 1982
52. Leem JW, Willis WD, Weller SC, Chung JM: Differential activation and classification of cutaneous afferents in the rat. *J Neurophysiol* 70:2411-2424, 1993
53. Levey AI, Kitt CA, Simonds WF, Price DL, Brann MR: Identification and localization of muscarinic acetylcholine receptor proteins in brain with subtype-specific antibodies. *J Neurosci* 11:3218-3226, 1991
54. Levin ED, McClernon FJ, Rezvani AH: Nicotinic effects on cognitive function: Behavioral characterization, pharmacological specification, and anatomic localization. *Psychopharmacology (Berl.)* 184:523-539, 2006
55. Levy RB, Reyes AD, Aoki C: Nicotinic and muscarinic reduction of unitary excitatory postsynaptic potentials in sensory cortex; dual intracellular recording in vitro. *J Neurophysiol* 95:2155-2166, 2006
56. Mesulam MM, Mufson EJ: Neural inputs into the nucleus basalis of the substantia innominata (ch4) in the rhesus monkey. *Brain* 107:253-274, 1984
57. Mesulam MM, Mufson EJ, Wainer BH, Levey AI: Central cholinergic pathways in the rat: An overview based on an alternative nomenclature (Ch1-Ch6). *Neuroscience* 10:1185-1201, 1983
58. Metherate R: Nicotinic acetylcholine receptors in sensory cortex. *Learn Mem* 11:50-59, 2004
59. Metherate R, Ashe JH: Basal forebrain stimulation modifies auditory cortex responsiveness by an action at muscarinic receptors. *Brain Res* 559:163-167, 1991
60. Muir JL, Page KJ, Sirinathsinghi DJS, Robbins TW, Everitt BJ: Excitotoxic lesions of basal forebrain cholinergic neurons: Effects on learning, memory and attention. *Behav Brain Res* 57:123-131, 1993
61. Nakayama H, Shioda S, Nakajo S, Ueno S, Nakashima T, Nakai Y: Immunocytochemical localization of nicotinic acetylcholine receptor in the rat cerebellar cortex. *Neurosci Res* 29:233-239, 1997
62. Neafsey EJ, Bold EL, Haas G, Hurley-Gius KM, Quirk G, Sievert CF, Terreberry RR: The organization of the rat motor cortex: A microstimulation mapping study. *Brain Res Rev* 11:77-96, 1986
63. Nunez A, Dominguez S, Buno W, Fernandez de Sevilla D: Cholinergic-mediated response enhancement in barrel cortex layer V pyramidal neurons. *J Neurophysiol* 108:1656-1668, 2012
64. Oldford E, Castro-Alamancos MA: Input-specific effects of acetylcholine on sensory and intracortical evoked responses in the "barrel cortex" in vivo. *Neuroscience* 117:769-778, 2003
65. Paré M, Smith AM, Rice FL: Distribution and terminal arborizations of cutaneous mechanoreceptors in the glabrous finger pads of the monkey. *J Comp Neurol* 445:347-359, 2002
66. Parikh V, Sarter M: Cholinergic mediation of attention: Contributions of phasic and tonic increases in prefrontal cholinergic activity. *Ann N Y Acad Sci* 1129:225-235, 2008
67. Pawson L, Prestia LT, Mahoney GK, Güçlü B, Cox PJ, Pack AK: GABAergic/Glutamatergic-Glial/Neuronal interaction contributes to rapid adaptation in pacinian corpuscles. *J Neurosci* 29:2695-2705, 2009
68. Paxinos G, Watson C: *The Rat Brain in Stereotaxic Coordinates*, 3rd ed. Academic Press, 1997
69. Pei YC, Denchev PV, Hsiao SS, Craig JC, Bensmaia SJ: Convergence of submodality-specific input onto neurons in primary somatosensory cortex. *J Neurophysiol* 102:1843-1853, 2009
70. Picciotto MR, Higley MJ, Mineur YS: Acetylcholine as a Neuromodulator: cholinergic signaling shapes nervous system function and behavior. *Neuron* 76:116-129, 2012
71. Pinto L, Goard MJ, Estandian D, Xu M, Kwan AC, Lee SH, Harrison TC, Feng G, Dan Y: Fast modulation of visual perception by basal forebrain cholinergic neurons. *Nat Neurosci* 16:1857-1863, 2013
72. Raggenbass M, Bertrand D: Nicotinic receptors in circuit excitability and epilepsy. *J Neurobiol* 53:580-589, 2002
73. Rasmusson DD: The role of acetylcholine in cortical synaptic plasticity. *Behav Brain Res* 115:205-218, 2000
74. Rasmusson DD, Smith SA, Semba K: Inactivation of prefrontal cortex abolishes cortical acetylcholine release evoked by sensory or sensory pathway stimulation in the rat. *Neuroscience* 149:232-241, 2007

75. Roberts MJ, Zinke W, Guo K, Robertson R, McDonald JS, Thiele A: Acetylcholine dynamically controls spatial integration in marmoset primary visual cortex. *J Neurophysiol* 93:2062-2072, 2005
76. Sahin M, Bowen WD, Donoghue JP: Location of nicotinic and muscarinic cholinergic and μ -opiate receptors in rat cerebral neocortex: Evidence from thalamic and cortical lesions. *Brain Res* 579:135-147, 1992
77. Sarter M, Givens B, Bruno JP: The cognitive neuroscience of sustained attention: Where top-down meets bottom-up. *Brain Res Brain Res Rev* 35:146-160, 2001
78. Sihver W, Gillberg PG, Nordberg A: Laminar distribution of nicotinic receptor subtypes in human cerebral cortex as determined by [3H](-)nicotine, [3H]cytisine and [3H]epibatidine in vitro autoradiography. *Neuroscience* 85:1121-1133, 1998
79. Sillito AM, Kemp JA: Cholinergic modulation of the functional organization of the cat visual cortex. *Brain Res* 289:143-155, 1983
80. Skieterska K, Rondou P, Van Craenenbroeck K: Regulation of G protein-coupled receptors by ubiquitination. *Int J Mol Sci* 18:923, 2017
81. Steinlein OK, Mulley JC, Propping P, Wallace RH, Phillips HA, Sutherland GR, Scheffer IE, Berkovic SF: A missense mutation in the neuronal nicotinic acetylcholine receptor $\alpha 4$ subunit is associated with autosomal dominant nocturnal frontal lobe epilepsy. *Nat Genet* 11:201-203, 1995
82. Tian MK, Bailey CDC, Lambe EK: Cholinergic excitation in mouse primary vs. associative cortex: Region-specific magnitude and receptor balance. *Eur J Neurosci* 40:2608-2618, 2014
83. Tribollet E, Bertrand D, Marguerat A, Raggenbass M: Comparative distribution of nicotinic receptor subtypes during development, adulthood and aging: An autoradiographic study in the rat brain. *Neuroscience* 124:405-420, 2004
84. Trinka E, Cock H, Hesdorffer D, Rossetti AO, Scheffer IE, Shinnar S, Shorvon S, Lowenstein DH: A definition and classification of status epilepticus-Report of the ILAE task force on classification of status epilepticus. *Epilepsia* 56:1515-1523, 2015
85. Turchi J, Sarter M: Cortical acetylcholine and processing capacity: Effects of cortical cholinergic deafferentation on crossmodal divided attention in rats. *Cogn Brain Res* 6:147-158, 1997
86. Turnbull IM, McGeer PL, Beattie L, Calne D, Pate B: Stimulation of the basal nucleus of meynert in senile dementia of alzheimer's type. *Stereotact Funct Neurosurg* 48:216-221, 1985
87. Vardar B, Guclu B: Effects of basal forebrain stimulation on the vibrotactile responses of neurons from the hindpaw representation in the rat SI cortex. *Brain Struct Funct* 225:1761-1776, 2020
88. Vardar B, Guclu B: Non-NMDA receptor-mediated vibrotactile responses of neurons from the hindpaw representation in the rat SI cortex. *Somatosens Mot Res* 34:189-203, 2017
89. Wu J, Lukas RJ: Naturally-expressed nicotinic acetylcholine receptor subtypes. *Biochem Pharmacol* 82:800-807, 2011
90. Xiang Z, Huguenard JR, Prince DA: Cholinergic switching within neocortical inhibitory networks. *Science* 281:985-988, 1998
91. Yusufogullari S, Kilinc D, Vardar B, Guclu B: Histological study of layer thickness in different cortical areas in rat. In: 2015 19th National Biomedical Engineering Meeting (BIYOMUT) Istanbul:IEEE, 2015
92. Zilles K, Palomero-Gallagher N: Multiple transmitter receptors in regions and layers of the human cerebral cortex. *Front Neuroanat* 11:1-26, 2017